

Efficient Control-Volume Model of the Compressible Euler equations

Xi Chen¹, Natalia Andronova¹, Bram Van Leer¹, Joyce E. Penner¹, S-J. Lin²,
John Boyd¹, Christiane Jablonowki¹, Quentin Stout¹

¹University of Michigan, ²NOAA Geophysical Fluid Dynamics Laboratory

Abstract:

In this paper we present a new nonhydrostatic dynamical core for a cloud-resolving model, which represents an extension of the finite-volume model with the Lin-Rood hydrostatic core using a generalized Lagrangian vertical coordinate. Both stable and accurate solutions were obtained by solving Riemann problems on all cell interfaces. Our scheme is approximately 30% more efficient than that of the ASUM⁺-up scheme. We tested this dynamical core on a few bubble tests. We also tested whether we are able to produce seamless solutions that span the hydrostatic and nonhydrostatic regimes using a gravity wave test.

1. Introduction

A critical requirement for improving global climate models (GCMs) is the development of fast and accurate schemes for treating convection and cloud formation. Progress in the development of GCMs that can accurately treat large-scale cloud formation and dynamics has been slow. This is partly because cloud formation is a subgrid-scale process that occurs under nonhydrostatic conditions in GCMs, which typically adopt the hydrostatic approximation. Global models that aim to resolve motions with a vertical scale of order 100 m need to include nonhydrostatic effects (Daley, 1988). However, the nonhydrostatic equations allow the development of fast sound waves, which can travel in all directions, vertically and horizontally and require special computational approaches (Durrán, 1989; Skamarock and Klemp, 1992) and/or small time steps in order to obtain accurate solutions. Therefore, the main question that faces the development of nonhydrostatic models is how to formulate an efficient numerical scheme for the small-scale processes represented in the nonhydrostatic atmosphere, which can correctly and stably represent the important atmospheric interactions at the model resolution (Skamarock, 2008).

Future climate models based on high-performance parallel computing paradigms will be able to address these questions based on first principles. On the one hand, they will enable us to further refine the model resolution on a global scale. On the other hand, they will allow improved physical parameterization (or a more exact treatment of physical processes) using adaptive grid methods. In addition, nonhydrostatic regions embedded in a hydrostatic model become feasible (Côté et al. 1998).

In our work, the NCAR Finite-Volume Community Atmospheric Model framework (FVCAM; first available as an option in CAM3) was used to develop the means to solve the problem of resolving cloud formation within a larger scale GCM. Our methods use techniques developed for adaptation of grid resolution. Solution adaptation is a powerful tool that has now been extended by our team at the University of Michigan to solve the equations of motion on a sphere for hydrostatic configurations. In addition, we have

added vertical adaptation as well as the ability to develop vertical integrals to the ABLCarT computational library. We also developed algorithms for merging the hydrostatic and nonhydrostatic flows when these two domains are joined.

In this paper we present results from a nonhydrostatic extension for the Lin-Rood dynamical core (Lin and Rood, 1996, 1997; Lin 2004) using a generalized Lagrangian vertical coordinate. The multidimensional flux-form semi-Lagrangian (FFSL) Lin-Rood dynamical core simulates the conservative, monotonic advection for prognostic variables and uses a “vertically Lagrangian” finite-volume (FV) representation of the model equations with a mass conserving re-mapping algorithm. The Lagrangian coordinate requires a remapping to restore the original resolution and keep the mesh from developing distortions such as layers with overlapping interfaces. The horizontal numerical algorithm of the Lin-Rood dynamical core is based on the C-D grid. This FFSL FV algorithm has been adopted in several atmospheric transport models (e.g., CAM, GFDL). We use an unstaggered grid and build the method so it does not require filtering of the acoustic waves. We test the method based on both an Eulerian and a Lagrangian formulation, using the 2-D warm bubble tests of Robert (1993) as well as his warm and cold interacting bubble test. We also test whether the results of this model can be merged with solutions in a pure hydrostatic version of the model using the Skamarock and Klemp (1992) gravity wave test. In Section 2 we briefly present a 2D (x-z) version of the fully compressible Euler equations; in Section 3 we present the results for two warm bubble test cases from Robert (1993); in Section 4 we present the results of the gravity wave propagation test; in Section 5 we present some conclusions.

2. Nonhydrostatic Model

Our model equations are the fully compressible FV Euler conservation equations in the flux form with a vertical Lagrangian coordinate with the model layers being material impenetrable surfaces and the bottom layer following the surface terrain. In our numerical representation of the model equations, we use an unstaggered grid. We use a five-point interpolation scheme to calculate all grid cell interface values of each control volume, and we calculate the fluxes at the interfaces by solving the Riemann problem in both the horizontal and vertical directions. We developed a light-weight approximate Riemann solver (LWARS) to use in both the horizontal and vertical directions. We show that LWARS saves considerable computational time (up to 30%) in comparison with the advection upstream splitting method (AUSM⁺-up) (Liou, 2006; Ullrich et al., 2010) but retains its accuracy.

3. Bubble Tests

We tested our nonhydrostatic approach in solving the equations for the nonhydrostatic atmosphere using the two standard tests of Robert (1993). These tests are for two different warm bubbles: the “uniform” bubble and “Gaussian” bubble, both rising in an isentropic atmosphere within a closed box. The results of the experiment for different model resolutions are presented in Fig. 1. We applied the same spatial grid resolution of five and ten meters as in Robert (1993). The uniform bubble (two left columns in Fig. 1) at $dx = 10$ m looks more “diffusive” than that shown by Robert

(1993), but it looks “sharper” at $dx = 5$ m where the Kelvin–Helmholtz instability curls at the bubble edges are nicely resolved. For the Gaussian bubble (last right column in Fig. 1), the main differences at 18 min are visible in the configuration of the bubble “head.” The Kelvin–Helmholtz instability in the upper branch of the bubble is better resolved than is the lower one. The results obtained with our Riemann solver approximation for both types of bubble are closer to the results obtained with the ASUM⁺-up Riemann solver (Liou, 2006).

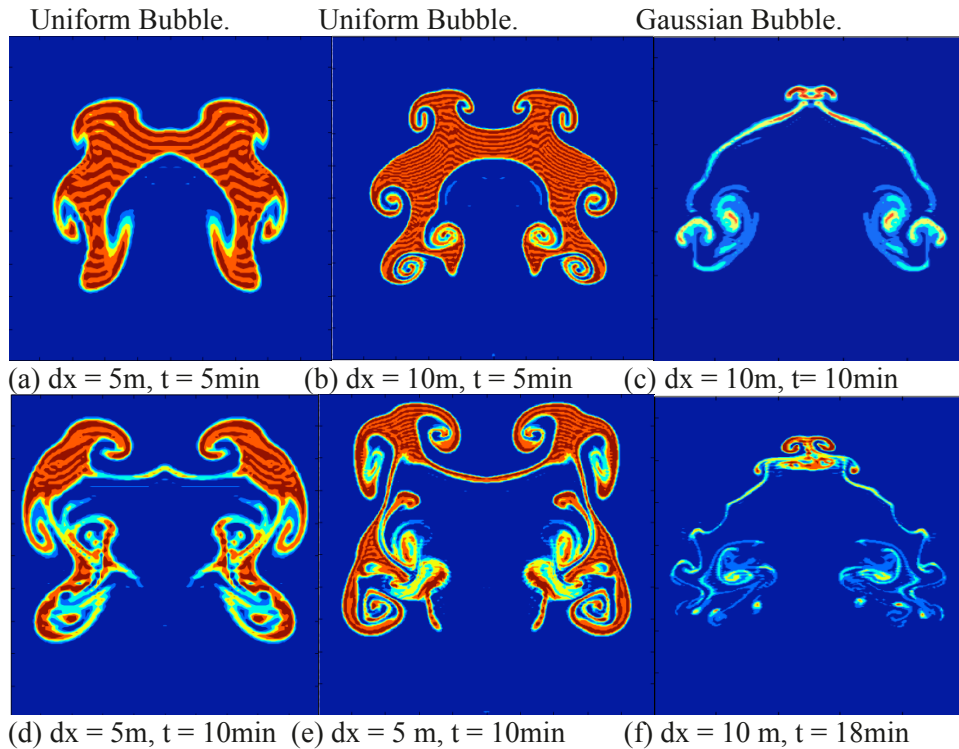


Figure 1. Uniform and Gaussian bubbles for different resolutions (dx,dz) and times (t).

4. Gravity Waves Propagation in Hydrostatic and Nonhydrostatic Regimes

We formulated the nonhydrostatic equations in a manner that would be consistent with a hydrostatic treatment based on a vertical Lagrangian coordinate, in order to be able to smoothly couple solutions between hydrostatic and nonhydrostatic regimes. Thus, we developed a version of the model that assumes the hydrostatic equations. In both the hydrostatic and nonhydrostatic codes, the flux form of the equations is used. Some variables, such as velocity components and potential temperature, are shared by both regimes; others, such as the nonhydrostatic pressure anomaly, are zero in the hydrostatic region and predicted in the nonhydrostatic region.

We used the gravity wave test from Skamarock and Klemp (1992) to test our ability to couple solutions in the hydrostatic and nonhydrostatic regimes in a one-layer configuration. This test was conducted in an atmosphere of constant Brunt-Väisälä frequency in a channel of length L and height H with an outgoing upper boundary and solid, free-slip lower boundary.

Figure 2 presents the test results at 50 min for the domain $L = 300$ km, $H = 10$ km with a disturbance located at 100 km. Each row in Fig. 2 represents different test resolutions: the upper row is 5000×500 m, the middle row is 2500×250 m and the last row is 1250×125 m. The first column represents a test where the initial perturbation started on the left in the hydrostatic regime and flows into the nonhydrostatic regime on the right (and also flows to the left, remaining in the hydrostatic regime). The right column represents a test where the initial perturbation starts on the left in the nonhydrostatic regime. In both columns, the initial disturbance is located on the left side of the white line, which separates the hydrostatic and nonhydrostatic regimes. In the first column the hydrostatic regime is on the left, while in the second column it is on the right. To link the two regions, we defined four additional ghost cells for our interpolation schemes in both regimes. These four ghost cells allow us to maintain a second-order accurate solution within both the hydrostatic and nonhydrostatic regimes with a minimum number of “ghost cell” overlap regions in the two regimes.

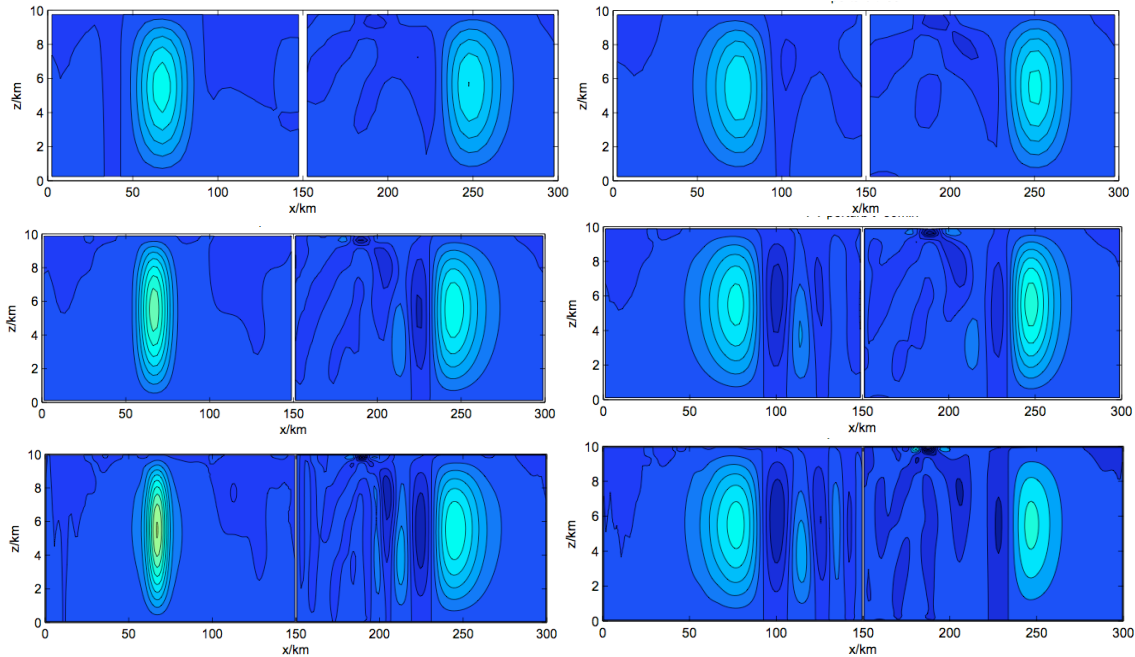


Figure 2. Transition from the hydrostatic to nonhydrostatic regime (left column) and from the nonhydrostatic to hydrostatic regime (right column) for different resolutions: Upper row is 5000×500 m, the middle row is 2500×250 m, and the last row is 1250×125 m (see further explanation in the text).

As expected, the coarse resolution results (first row) show a perturbation that looks similar in both hydrostatic and nonhydrostatic regimes. The high-resolution case (the last row) shows considerable differences in both the hydrostatic vs. nonhydrostatic gravity wave propagation and a different wave structure when the wave is propagating from the hydrostatic part to the nonhydrostatic part and also when it is propagating from the nonhydrostatic part to the hydrostatic part.

5. Conclusions

We have benchmarked our numerical solver's performance with a series of tests. Our solution technique is stable and does not amplify numerical noise during the integration. We are extending this dynamical core for eventual use in an adaptive mesh refinement version of a global dynamical core.

Acknowledgments. This work was supported through the DOE Scientific Discovery through Advanced Computing program Grant number DOE FG02 01 ER63248

References

- Côté, J, Gravel, A. Metot, A. Patoine, M. Roch, and A. Staniforth, 1998: The operational CMC/MRB Global Environmental Multiscale (GEM) model, Part I: Design considerations and formulation. *Mon. Wea. Rev.*, 126:1373–1395.
- Daley, R., 1988: The normal modes of the spherical non-hydrostatic equations with applications to the filtering of acoustic modes. *Tellus*, 40A, 96–106.
- Durrant, D. R., 1989: Improving the anelastic approximation. *J. Atmos. Sci.*, 46, 1453–1461
- Lin, S.-J., 2004: A “vertically Lagrangian” finite-volume dynamical core for global models. *Mon. Wea. Rev.*, 132, 2293–2307.
- Lin, S.-J. and R. Rood, 1996: Multidimensional flux-form semi Lagrangian transport schemes. *Mon. Wea. Rev.*, 124, 2046–2070.
- Lin, S.-J., and R. B. Rood, 1997: An explicit flux-form semi-Lagrangian shallow-water model on the sphere, *Q. J. R. Meteor. Soc.*, 123:2477–2498.
- Liou, M.-S., 2006: A sequel to AUSM, Part II: AUSM+-up. *J. Comput. Phys.*, Vol. 214, 137–170, 2006.
- Robert, A. J., 1993: Bubble convection experiments with a semi-implicit formulation of the Euler equations. *J. Atmos. Sci.*, 50, 1865–1873.
- Skamarock, W. C., and J. B. Klemp, 1992: The stability of time-split numerical methods for the hydrostatic and non-hydrostatic elastic equations, *Mon. Wea. Rev.* 120, 2109–2127.
- Skamarock, W. C., 2008: A linear analysis of the NCAR CCSM finite-volume dynamical core. *Mon. Wea. Rev.*, 136, 2112–2119.
- Smolarkiewicz, P. K., and L. G. Margolin, 1994: Variational solver for elliptic problems in atmospheric flows. *Appl. Math. Comp. Sci.*, 4, 527–551.
- Smolarkiewicz, P. K., and J. A. Pudykiewicz, 1992: A class of semi-Lagrangian approximations for fluids. *J. Atmos. Sci.*, 49, 2082–2096.
- Ullrich, P. A., C. Jablonowski, and B. van Leer, 2010: Riemann-solver-based high-order finite-volume models for the shallow-water equations on the sphere, *J. Comput. Phys.*, 229, 6104–6134.